

# ADUGS-VINS: Generalized Visual-Inertial Odometry for Robust Navigation in Highly Dynamic and Complex Environments

Rui Zhou<sup>1</sup>, Jingbin Liu<sup>2\*</sup>, Junbin Xie<sup>1</sup>, Jianyu Zhang<sup>1</sup>, Yingze Hu<sup>1</sup> and Jiele Zhao<sup>1</sup>

<sup>1</sup>Electronic Information School, Wuhan University

<sup>2</sup>State Key Laboratory of Information Engineering in Surveying, Mapping and Remote Sensing, Wuhan University

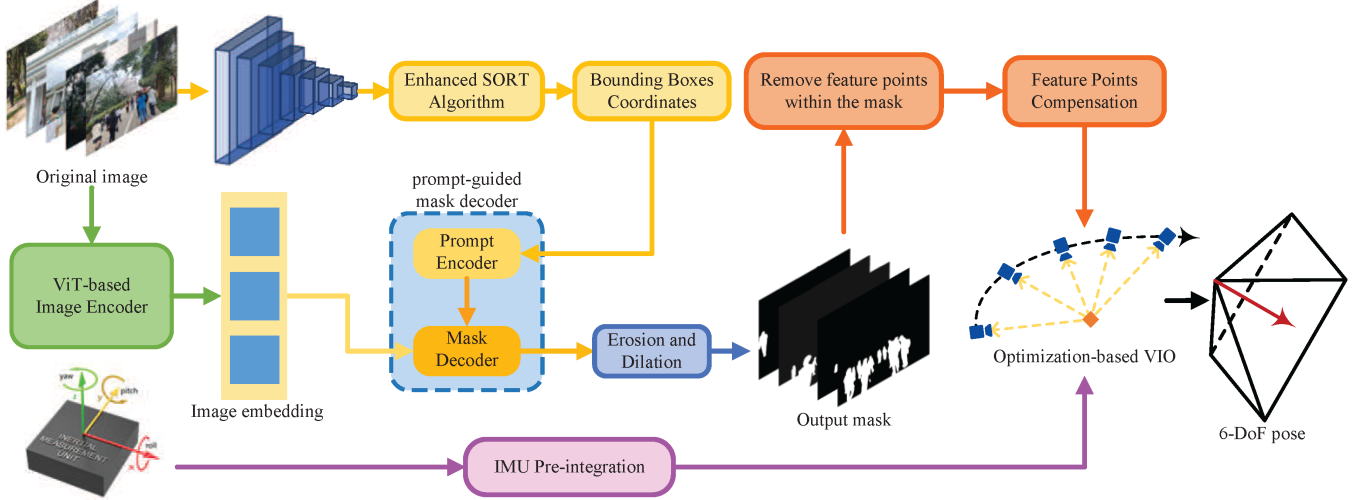


Fig. 1: Overview of ADUGS-VINS. Our method effectively segments various moving objects even under conditions of partial occlusion, demonstrating the efficacy of ADUGS-VINS in segmentation within complex environments.

**Abstract**—Visual-inertial odometry (VIO) is widely used in various fields, such as robots, drones, and autonomous vehicles. However, real-world scenes often feature dynamic objects, compromising the accuracy of VIO. The diversity and partial occlusion of these objects present a tough challenge for existing dynamic VIO methods. To tackle this challenge, we introduce ADUGS-VINS, which integrates an enhanced SORT algorithm along with a promptable foundation model into VIO, thereby improving pose estimation accuracy in environments with diverse dynamic objects and frequent occlusions. We evaluated our proposed method using multiple public datasets representing various scenes, as well as in a real-world scenario involving diverse dynamic objects. The experimental results demonstrate that our proposed method performs impressively in multiple scenarios, outperforming other state-of-the-art methods. This highlights its remarkable generalization and adaptability in diverse dynamic environments, showcasing its potential to handle various dynamic objects in practical applications.

## I. INTRODUCTION

Accurate motion estimation in unfamiliar scenarios is crucial for various vision and robotics applications, including augmented reality (AR), unmanned aerial vehicles (UAVs) and autonomous driving. Techniques like visual-inertial SLAM (VI-SLAM) and visual-inertial odometry (VIO) are broadly employed in this domain, serving as fundamental methods for numerous robotic applications that demand accurate positioning or navigation in environments where GNSS (Global Navigation Satellite System) signals are obstructed. Most current visual SLAM and VIO methods typically presume that observed objects remain static

and time-invariant. However, as a robot navigates in urban environments, moving objects like pedestrians and vehicle can adversely affect the precision of VIO system localization, causing a mismatch between anticipated and actual trajectory. Accordingly, solutions designed to reduce the influence of dynamic objects on estimation results is critical. To mitigate the impact of moving objects, researchers have incorporated semantic information to improve the performance of VIO systems in dynamic settings [1]–[3]. However, earlier studies into dynamic VIO solutions employing conventional models like SegNet [4] and Mask R-CNN [5] encountered limitations. These restrictions arose from their restricted generalization in segmenting varied moving objects and their inadequate performance in handling object segmentation in cases of partial occlusion. Consequently, existing methods become unreliable and imprecise in such dynamic environments, particularly under partial occlusion conditions, limiting their practical usability.

This work introduces ADUGS-VINS (Advanced Generalized Universal Dynamic Segmentation Visual-Inertial Odometry), a universally applicable VIO method designed for dynamic environments involving diverse moving objects, incorporating an innovative multi-category segmentation technique. Our approach leverages the powerful zero-shot generalization capability of the Segment Anything Model (SAM) [6] for multi-category segmentation tasks. Furthermore, we have developed an enhanced SORT algorithm based on Simple Online and Real-Time Tracking [7] to improve the

robustness of the target tracking model in complex urban environments, especially in cases of partial obstructions. Leveraging these two techniques, ADUGS-VINS can identify a range of moving objects in intricate, ever-changing settings, even amidst frequent partial blockages.

To verify the effectiveness and generalization of ADUGS-VINS in intricate dynamic settings, we conducted comprehensive experiments using various datasets with completely different scenarios and dynamic objects. We evaluate ADUGS-VINS against other state-of-the-art VIO methods [2], [3], [8]–[10], and the results show our approach excels across various scenarios, outperforming these state-of-the-art VIO methods. This underscores its exceptional generalization and adaptability in complex dynamic environments, highlighting its potential for managing dynamic objects in real-world applications. Ablation experiments are conducted to demonstrate the effectiveness of the proposed method. Regarding the enhanced SORT algorithm, accuracy in the VIODE dataset can be improved by up to 83.28%. In addition to testing on public VIO datasets, we also ran experiments on actual devices in challenging real-world dynamic scenarios, proving that our approach can effectively mitigate the impact of complex dynamic environments. The dataset collected in real-world environments is publicly available at ADUGS-VINS Dataset, providing a resource for the research community to dynamic VIO and related fields. Our main contributions are summarized as follows:

- We introduce an innovative VIO solution, ADUGS-VINS, designed for challenging dynamic conditions that exhibit exceptional adaptability and generalization in various environments.
- We employ an enhanced SORT algorithm alongside a promptable foundational model to accurately track and segment a variety of moving objects, thereby effectively reducing performance decreases in VIO within dynamic settings.
- Extensive experiments conducted on diverse public datasets and real-world scenarios demonstrate that ADUGS-VINS performs exceptionally well in varied environments, surpassing state-of-the-art methods in pose estimation accuracy.
- A large-scale visual-inertial dataset is presented, which differs from existing datasets by containing various dynamic characters throughout the sequences.

## II. RELATED WORKS

### A. Visual-Inertial Odometry

Recently, Visual Inertial Odometry (VIO) have become a research focus in the fields of robotics applications. Based on the method of the fusion of visual and inertial measurements, classic VIO systems are generally classified into filter-based and optimization-based categories. Filter-based methods [11]–[15] typically utilize the extended Kalman filter (EKF) for pose estimation. Optimization-centric approaches [8], [9], [9], [16]–[18] predominantly rely on the extraction of features and visual-inertial bundle adjustment

to obtain precise pose estimation. Learning-based methods in VIO [19]–[22], have also been explored in recent years, yielding encouraging outcomes.

Integrating IMU motion data allows VIO systems to resist interference from moving objects in the background to some extent. Nevertheless, their performance in highly dynamic scenarios is still restricted. Specifically, when dynamic regions dominate the camera view, both the accuracy and reliability of VIO are greatly reduced, resulting in discrepancies between estimated and actual trajectories or even localization failure.

### B. Dynamic Objects Removal in Visual and VI Odometry

In recent years, the use of visual methods to track dynamic objects has emerged as a prominent area of research. Fan et al. [23] and Sun et al. [24] put forth a multi-view geometry-based method that enhances RGB-D SLAM in dynamic environments. Tan et al. [25] presented a novel prior-based adaptive RANSAC algorithm (PARSAC) that effectively eliminates outliers, ensuring reliable camera pose estimation under dynamic conditions. Furthermore, some work is based on the structure of the plane, such as that presented in RP-VIO [26], which employs the simple geometry of planes to enhance robustness and accuracy in dynamic environments. RD-VIO [27] uses the IMU-PARSAC algorithm to robustly handle dynamic scenes. Most methods utilize motion priors from the IMU, allowing VIO to tolerate environments containing dynamic objects to some degree. However, when dynamic objects occlude a significant portion of the view, the issue cannot be solved solely by using the prior motion. [3]

In light of the advances of computer vision, researchers have integrated semantic information into VIO solutions aimed at addressing the constraints of approaches based on motion prior. Approaches such as DS-SLAM [1], DynaVINS [3], Mask-Fusion [28], Dynamic-VINS [2] and Dyna-SLAM [29] have integrated semantic segmentation methods, including SegNet [4] and Mask R-CNN [5], for the purpose of eliminating the effects of dynamic areas in the visual image.

Deep learning and pixel-level semantic segmentation yield significant outcomes in this area; however, they are restricted to the classes of segmented objects and conditions of partial occlusion. The limited generalizability of traditional segmentation models and their inadequacy in reducing the impact of moving objects with partial occlusions greatly impede their applicability in real-world scenarios. Although effective in specific environments, these methods suffer from accuracy and reliability under complex dynamic environmental conditions. Therefore, creating a universal segmentation technique to address these challenges for dynamic objects is essential for VIO applications in real-world situations.

## III. METHODOLOGY

This section details ADUGS-VINS method. We begin with the improved SORT algorithm and segmentation approach in section III-A, which is proficient in robust object segmentation across multiple categories in challenging environments.

Subsequently, section III-B describes the feature tracking and compensation techniques in our VIO method.

### A. Robust Tracking and Promptable semantic segmentation of multi-category dynamic objects

We present the improved SORT algorithm designed for stable tracking of potentially dynamic objects under partial occlusion conditions. Once the enhanced SORT algorithm is employed for tracking moving objects, the promptable foundation segmentation model is then used to identify moving components from static backgrounds at the pixel level.

Assuming that there are two adjacent frames  $i - 1$  th and  $i$  th frame. Initially we utilize s YOLOv11 [30] to process these frames in the video sequences, generating a bounding box for every potential dynamic objects. In order to ascertain which predicted box in the  $i$  th frame corresponds to a specific bounding box in the  $i - 1$  th frame, we introduce the Hungarian algorithm to obtain the optimal estimate of the correspondence between multiple bounding boxes of objects in the images of the previous and subsequent frames. Once the correspondence of the bounding boxes has been established, the bounding box corresponding to any given box in a previous frame can be identified. Consequently, the Kalman filter [31] can be updated based on the previous state. For each bounding box, the state of the bounding box is defined as follows:

$$\hat{\mathbf{x}} = [x \quad y \quad w \quad h \quad v_x \quad v_y \quad v_w \quad v_h]^\top \quad (1)$$

In the state equation, the variables  $x$  and  $y$  represent the target center position,  $w$  and  $h$  represent the length and width of the bounding boxes,  $v_x$  and  $v_y$  represent the speed of movement of the target center position,  $v_w$  and  $v_h$  represent the time rate of change of the length and width of the bounding boxes.

Measurement noise covariance matrices  $\mathbf{R}$  are vital for the Kalman filter to accurately estimate dynamic states. Traditional methods for estimating these matrices are often inadequate for optimal filtering. [32] We propose an adaptive filtering method that dynamically estimates the measurement noise covariance matrix,  $\mathbf{R}$ , by analyzing residuals to enhance the Kalman filter's state estimation. This process utilizes a sliding window to collect residuals, computed using the function given below:

$$\delta_k = [\delta_x \quad \delta_y \quad \delta_w \quad \delta_h]_k = \mathbf{z}_k - \mathbf{H} \cdot \hat{\mathbf{x}}_{k|k-1} \quad (2)$$

Where  $\delta_x, \delta_y, \delta_w, \delta_h$  represents the residuals vector, it quantifies discrepancies between the actual measurements  $\mathbf{z}_k$  and the predictions from the Kalman filter.  $\mathbf{H}$  represents the measurement matrix, which maps the predicted state  $\hat{\mathbf{x}}_{k|k-1}$  to the measurement space. We calculate the  $\delta_{RMSE}$  of the residuals in the sliding window of  $N$  frames, which provides a robust measure of the magnitude of the residuals, reflecting the average error magnitude over the sliding window,

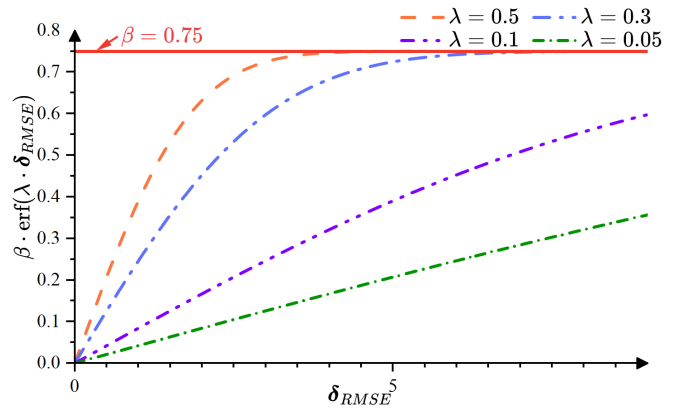


Fig. 2: Changes of measurement noise covariance matrix updating function w.r.t. parameter  $\lambda$ .

computed as :

$$\delta_{RMSE} = \left( \frac{1}{N} \sum_{i=1}^N (\delta_i)^2 \right)^{\frac{1}{2}} \quad (3)$$

This metric reflects the present variability in measurement noise, providing a real-time view of deviations from anticipated behavior. Once the RMSE values are acquired, the measurement noise covariance matrix  $\mathbf{R}$  is adaptively revised by applying a transformation to  $\delta_{RMSE}$ . The measurement noise covariance matrix updating function is determined as

$$\mathbf{R} = \text{diag} (\beta \cdot \text{erf}(\lambda \cdot \delta_{RMSE})) \quad (4)$$

Where  $\text{erf}(x)$  is the error function, which defined as:

$$\text{erf}(x) = \frac{2}{\sqrt{\pi}} \int_0^x e^{-t^2} dt \quad (5)$$

The parameters  $\lambda$  and  $\beta$  play pivotal roles in shaping the behavior of our function:  $\lambda$  modulates the steepness of the function's transition, while  $\beta$  determines the output's magnitude. The error function generates a smooth S-shaped curve that adeptly scales RMSE values, fostering stable and reliable filter behavior. Such smoothness is crucial for managing real-world data, particularly when dealing with outliers or noise, as it reduces the risk of the filter overreacting to these anomalies. Additionally, the function is designed to restrictively limit the impact of large residuals, thereby protecting against abrupt and significant alterations to  $\mathbf{R}$ . Utilizing a sliding window and error function scaling, this method adapts to measurement noise variations while maintaining estimation stability. It allows the Kalman filter to optimize performance by adjusting parameters based on real-time accuracy and reliability, resulting in more precise state estimations under varying conditions. Subsequently, the predicted bounding boxes from adaptive Kalman filtering are used to rectify deficiencies in the original target detection model. This approach addresses multiple object tracking instability effectively, significantly enhancing the robustness and accuracy of dynamic object tracking in complex environments.

After the adaptive Kalman filtering method, The coordinates of these bounding boxes are then used to guide

promptable foundation model in segmenting objects within the camera’s field of view. In order to enhance the real-time performance of the method, we employ Mobile SAM as a promptable foundation model, which is more time-efficient and consumes fewer computational resources. Mobile SAM will perform segmentation focusing on the object that occupies the majority of the area delineated by these coordinates. This method ensures precise segmentation of moving objects tracked by the SORT algorithm, creating a mask that differentiates dynamic from static regions.

Furthermore, to enhance the mask quality, we further refine it through erosion and dilation processes. We opted for a circular structure in processing the mask because it effectively preserves the original shape and details while minimizing the risk of distortion. The initial step involves denoising the mask using an erosion algorithm, which can effectively eliminate the small noise spots present in the mask. Assuming that the original mask is  $\mathbf{M}_{original}$ , the structure used for erosion is  $\mathbf{S}_{erode}$  and the eroded mask is  $\mathbf{M}_{erode}$ :

$$\begin{aligned} \mathbf{M}_{erode} &= \mathbf{M}_{original} \ominus \mathbf{S}_{erode} \\ &= \{x, y | (\mathbf{S}_{erode})_{xy} \subseteq \mathbf{M}_{original}\} \end{aligned} \quad (6)$$

The mask is further dilated to guarantee that the mask’s dynamic region fully encompasses the object, preventing the extraction of feature points along the object’s edges during feature extraction. Assuming the dilated mask  $\mathbf{M}_{dilate}$  and the dilation structure is  $\mathbf{S}_{dilate}$ . To eliminate the impact of mask reduction during erosion operations, one must ensure  $\mathbf{S}_{dilate} > \mathbf{S}_{erode}$ :

$$\begin{aligned} \mathbf{M}_{dilate} &= \mathbf{M}_{erode} \oplus \mathbf{S}_{dilate} \\ &= \{x, y | (\mathbf{S}_{dilate})_{xy} \cap \mathbf{M}_{erode} \neq \emptyset\} \end{aligned} \quad (7)$$

Through erosion and dilation processing, noise can be effectively eliminated, and the edges of dynamic regions can be covered without distorting the original mask, in preparation for feature point removal.

### B. Robust feature tracking and optimization for VIO in dynamic scenes

The approach outlined in section III-A allows us to achieve semantic segmentation for dynamic objects, enabling us to filter out moving feature points based on segment masks. ADUGS-VINS employs KLT sparse optical flow [33] to track these feature points across frames. During this process, any points within the segmented area are tagged as dynamic and consequently discarded. New feature points are detected using the ORB algorithm [34] in the unmasked regions of the image. To ensure a robust distribution of feature points and keep a sufficient count of static points for precise pose estimation, we optimize feature point detection through Adaptive Non-maximal Suppression (ANMS) [35], which balances strength and spatial distribution of feature points. Additionally, a compensation strategy is applied to

maintain an adequate number of feature points for precise pose estimation before bundle adjustment.

Denote  $\mathcal{K}$  as the set of ORB keypoints, with  $N_{max}$  as the maximum number of feature points and  $D_{min}$  as the minimum distance between them. Every feature point  $k_i$  is associated with a suppression radius  $\rho_i$ , expressed as:

$$\rho_i = \min\{\|\mathbf{p}_i - \mathbf{p}_j\| \mid r_j > r_i\} \quad (8)$$

where  $\mathbf{p}_i$  and  $\mathbf{p}_j$  are the positions of key points  $k_i$  and  $k_j$ , respectively, and  $r_i$  and  $r_j$  are their corresponding response values. Feature points are ranked by  $\rho_i$  in descending order, and the top  $N_{max}$  keypoints with the greatest suppression radius are selected. Subsequently, utilize  $D_{min}$  to filter feature points, ensuring that the spacing between two is not less than  $D_{min}$ . This method guarantees a consistent spatial distribution of high-quality features throughout the image.

Additionally, a compensation strategy is applied to maintain sufficient feature points for accurate pose estimation. The points tracked in the previous frame and the newly detected feature points in the  $m$  th frame are regarded as the set  $\mathcal{K}_m$ . The  $n$  th feature point is denoted as point  $k_m^n$ . The set of feature points detected in the  $i-1$  th frame can be expressed as:

$$\mathcal{K}_{i-1} = \{k_{i-1}^1, k_{i-1}^2, \dots, k_{i-1}^{n-1}, k_{i-1}^n\} \quad (9)$$

For optical flow matching between frame  $i-1$  and frame  $i$ , the points in  $\mathcal{K}_{i-1}$  that align in frame  $i$  are denoted as  $j_i^1, j_i^2, \dots, j_i^s$ . Given the altered positions of objects between the frames, we traverse the points  $j_i^1, j_i^2, \dots, j_i^s$  to determine whether they fall within the mask’s dynamic region; if they do, the points are excluded.

Assume that  $r$  points are excluded in this process, leaving  $s-r$  points denoted as  $j_i^1, j_i^2, \dots, j_i^{s-r-1}, j_i^{s-r}$ , a new round of static feature point extraction should be performed in the  $i$  th frame. In this iteration of the feature point extraction process, the maximum number of points to be extracted is set to  $N_{max} - s + r$  for compensation. This guarantees that ADUGS-VINS has an adequate number of reliable static feature points for pose calculation, ensuring that the system can continue to operate stably even when the area of dynamic regions in the image is extensive. This enhances the robustness of ADUGS-VINS in complex dynamic environments. Suppose that  $r$  points are omitted during this procedure, resulting in  $s-r$  points represented as  $j_i^1, j_i^2, \dots, j_i^{s-r-1}, j_i^{s-r}$ . In the newly  $i$ th frame, a fresh iteration of static feature point extraction is executed. During this iteration, the maximum number of extractable points is determined as  $N_{max} - s + r$  to ensure compensation. This approach guarantees that ADUGS-VINS retains an adequate number of reliable static feature points for precise pose estimation, thus enabling the system to maintain stable operation even when a significant portion of the image is in motion.

Method	VIODE											
	City day				City night				Parking lot			
	none	low	mid	high	none	low	mid	high	none	low	mid	high
ORB-SLAM3 [8]	2.179	5.301	2.204	*	0.176	*	*	*	0.287	2.897	6.742	7.482
VINS-Fusion [9]	0.203	0.148	0.261	0.321	0.319	0.368	0.433	0.490	0.120	0.113	0.161	1.201
VINS-Mono [17]	0.186	0.237	0.263	3.169	0.314	0.436	0.727	0.575	0.102	0.109	2.915	4.933
RP-VIO [26]	0.382	0.229	0.435	0.536	0.263	0.509	0.652	0.577	0.981	1.334	0.375	0.713
Dyna-VINS [3]	0.349	0.330	0.258	0.245	0.687	0.207	0.251	0.311	0.046	0.106	0.118	0.107
<b>ADUGS-VINS (Ours)</b>	<b>0.107</b>	<b>0.156</b>	<b>0.138</b>	<b>0.244</b>	<b>0.125</b>	<b>0.246</b>	<b>0.222</b>	<b>0.217</b>	<b>0.099</b>	<b>0.160</b>	<b>0.204</b>	<b>0.094</b>

• \*: Failure case.

TABLE I: Comparison with State-of-the-art Methods (RMSE of ATE in [M]). We highlight the top two results of each column in red and purple.

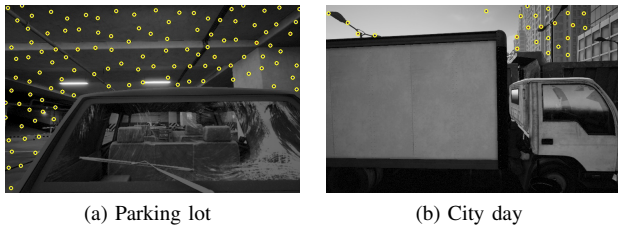


Fig. 3: Feature points distribution of ADUGS-VINS in VIODE dataset. The truck in fig. 3a exhibits a partial occlusion relationship. A significant portion of the car in fig. 3b is outside the field of camera view.

#### IV. EXPERIMENTAL RESULT

We conducted comparative experiments using public VIO datasets to assess the improvements of ADUGS-VINS in dynamic settings, comparing its performance against the state-of-the-art method in the field.

##### A. Dataset

The VIODE [36] and OpenLORIS-Scene [37] datasets were selected for the evaluation of VIO solutions. VIODE [36] is a synthetic dataset captured from an aerial drone, containing sequences from three environments. It is important to note that the subsequence nomenclature, ranging from 'none' to 'high,' denotes the dynamic level of the scene. The OpenLORIS-Scene dataset [37] includes a mix of visual, inertial, and odometric data from typical environments such as offices, homes, and commercial settings. It encompasses real-world challenges like changing lighting and moving individuals, closely resembling the everyday dynamic conditions. While VIODE centers on outdoor scenes with dynamic traffic scenarios, OpenLORIS encompasses various indoor scenes. These datasets were selected to evaluate the versatility of the VIO solution in different environmental conditions with varying dynamic objects.

##### B. Evaluation on VIODE Dataset

1) *ATE Comparison on VIODE Dataset:* In our study, we conducted an evaluation of existing Visual-Inertial Odometry (VIO) algorithms using the VIODE dataset. The outcomes of these evaluations are detailed in table I. Previous methods have proven effective in accurately estimating poses within static environments or in situations where there are only a few dynamic objects. However, as the prevalence of dynamic

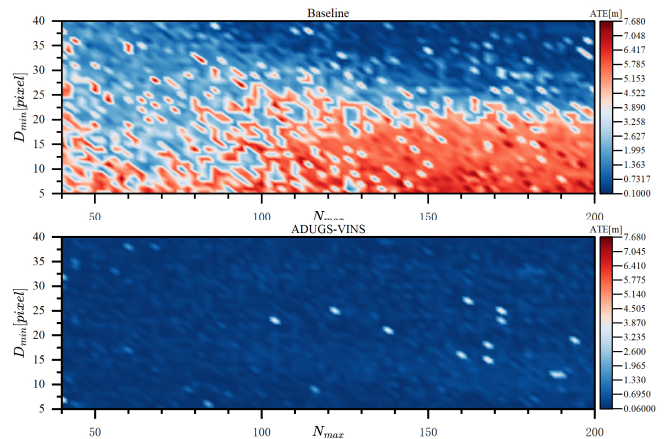


Fig. 4: The heatmap illustrates RMSE ATE in relation to the maximum feature points  $N_{max}$  and minimum feature point distance  $D_{min}$  for the "high" sequence within the parking lot environment of the VIODE dataset. The color bar represents the range of ATE values.

objects increases, particularly when they dominate the camera's field of view, the performance of these algorithms tends to decline markedly, resulting in notable deviations in trajectory calculations. In comparison to other methodologies, our proposed approach exhibits superior performance, especially in terms of RMSE of the absolute trajectory error (ATE) within the "high" sequence category of VIODE. Moreover, the experiment shows that ADUGS-VINS can efficiently manage not only partial occlusions, as illustrated in fig. 3a, but also situations where most dynamic objects are out of the field of view, as presented in fig. 3.

2) *Ablation Study of the Segmentation Workflow:* To illustrate the impact of the segmentation process within ASDUGS-VINS on reducing the effects of dynamic objects, we carried out ablation studies using different combinations of maximum feature points  $N_{max}$  and minimum feature point separation  $d_{min}$  in VIO to model varying feature point densities. fig. 6 depict the outcomes. Our method demonstrates superior accuracy across various  $N_{max}$  and  $d_{min}$  configurations. The baseline's accuracy is severely impacted by  $N_{max}$  and  $d_{min}$ , lacking robustness and stability. Conversely, ADUGS-VINS demonstrates low RMSE ATE across the entire heatmap, indicating not only exceptional precision in dynamic pose estimation but also remarkable robustness and stability.



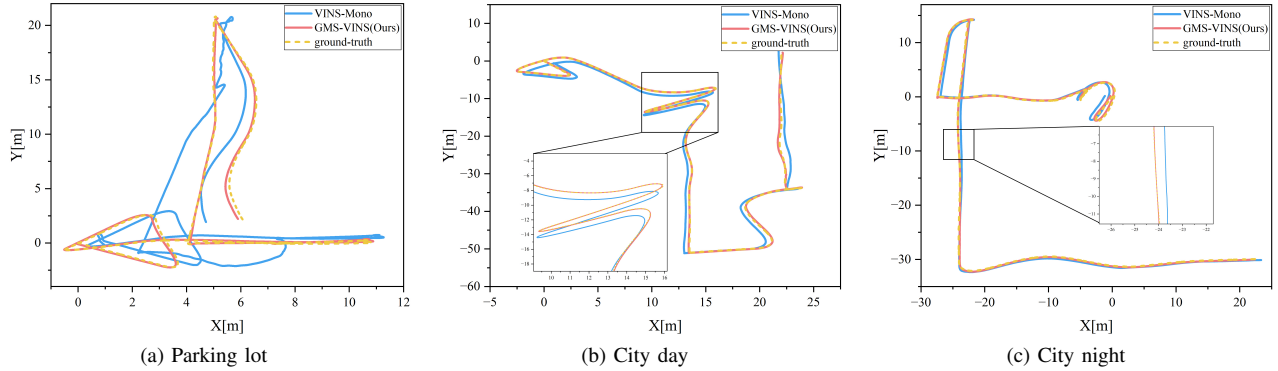


Fig. 5: A comparison of the trajectories of various VIO system on the “high” sequence of the VIODE dataset is presented. The ground truth is highlighted with a dashed yellow line. It can be observed that the trajectory obtained by ADUGS-VINS is the most accurate, with a high degree of overlap with the ground truth, reflecting the precision of the algorithm.

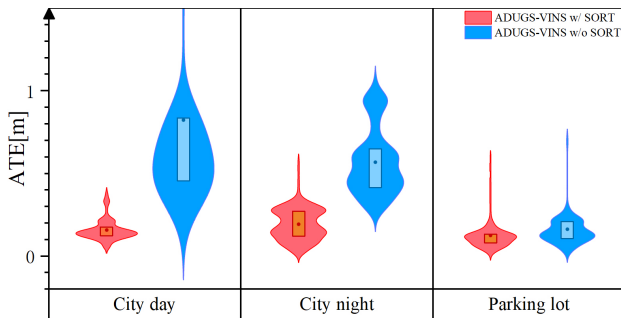


Fig. 6: Results of the ablation experiment for the enhanced SORT algorithm in ADUGS-VINS. This figure illustrates the ATE distribution for ADUGS-VINS in two configurations: including SORT (red) and excluding SORT (blue).

3) *Ablation Experiment for the Enhanced SORT algorithm*: To further assess the effectiveness of the improved SORT algorithm within ADUGS-VINS, we performed an ablation experiment to examine its impact on ADUGS-VINS precision in dynamic environments.

As demonstrated in fig. 6, the experimental data substantiates that the implementation of the SORT algorithm in the inertial visual odometry system notably enhances the positioning accuracy. In the parking lot scenario, the algorithm reduced the RMSE ATE by 21.38%. More substantial improvements were observed in urban settings, with an 83.28% reduction during daytime and a 63.99% reduction at night. These results indicate that our enhanced SORT algorithm significantly boosts ADUGS-VINS performance in challenging environments with a more effective state estimation approach. Particularly in scenarios with substantial alterations in illumination or occlusion relationships that result in inadequate visual data, the algorithm can effectively bolster the stability and precision of target tracking, minimize the deviations of inertial visual odometry, and reinforce the robustness and accuracy of the ADUGS-VINS system.

### C. Evaluation on OpenLORIS Dataset

To assess the generalizability of our approach, we conducted experiments using the challenging OpenLORIS dataset [37], which primarily features large-scale in-

door scenes. Despite using RMSE ATE, the Correct Rate (CR) [37] is used as a metric to assess the robustness over the whole data period. The results of the experiment are depicted in fig. 7. Our approach drastically outperforms existing VIO techniques in market environments, superior in both RMSE ATE and accuracy rate. The market scenario (figs. 8a and 8b) in OpenLORIS features the highest variety and quantity of dynamic objects, recorded in a supermarket full of people and shopping carts. Consequently, ADUGS-VINS is demonstrated to be effective in challenging dynamic environments. In corridor scenes within the dataset, many methods struggle due to featureless walls and low-light conditions, which result in loss of tracking. However, due to the robust feature tracking and optimization detailed in section III-B, ADUGS-VINS exceeds other methods in terms of both accuracy and robustness, demonstrating its universality and adaptability in challenging environments. In other sequences, which contain fewer static objects and less challenging environments, ADUGS-VINS attains a competitive performance compared to state-of-the-art methods.

### D. Experiment in real-world scenarios

In addition to validating our approach on public datasets, we also performed experiments in real-world settings. A RealSense D435i camera captures visual and inertial data for monocular visual-inertial SLAM. We collected an extensive outdoor dataset featuring a variety of moving objects, including pedestrians, cars, buses, motorcycles, and tricycles. fig. 9 presents the alignment of the estimated and ground-truth trajectories with satellite images from Microsoft. In these complex environments, ADUGS-VINS demonstrated robust and stable pose estimation with minimal drift compared to the baseline method.

## V. DISCUSSION AND CONCLUSION

This study presents ADUGS-VINS, an innovative VIO method that provides excellent accuracy in diverse and challenging dynamic environments. ADUGS-VINS employs a promptable foundation model to boost the generalization of dynamic object segmentation and uses an advanced SORT

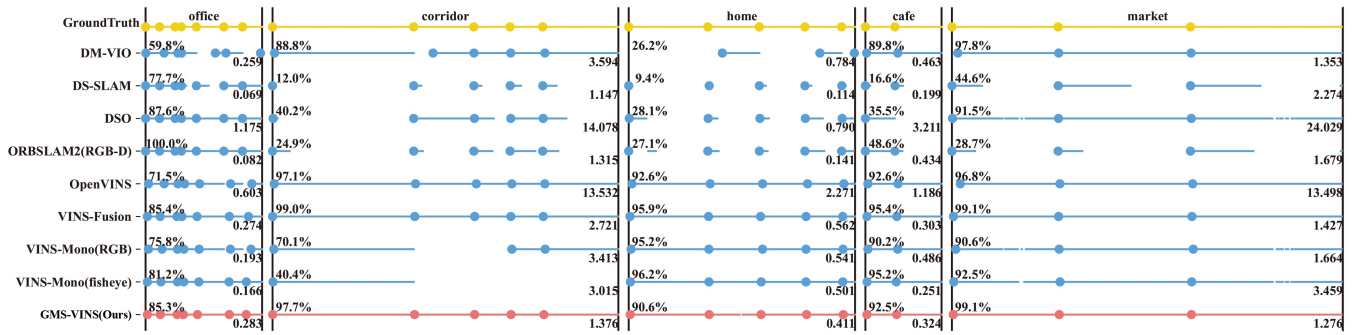


Fig. 7: Experiment results with the OpenLORIS-Scene datasets. For every algorithm, the dots represent successful initiation instances, and the lines show the span of successful tracking. The percentage in the top left corner of each scene indicates the average correct rate; a higher correct rate suggests greater algorithm robustness. The float value on the first line below depicts the average ATE RMSE, with lower values indicating higher accuracy. Some experimental results from prior methods are referenced from [37]

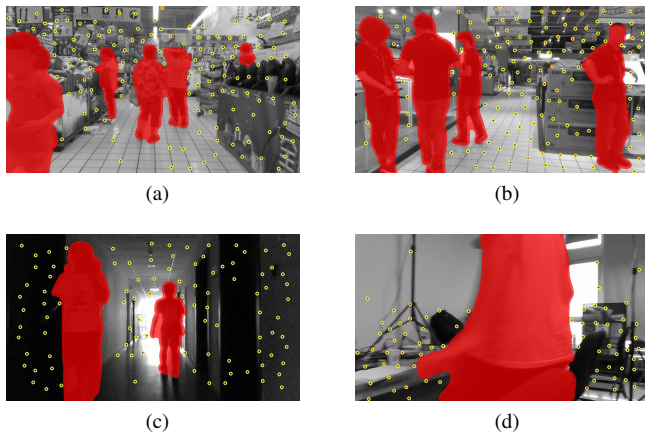


Fig. 8: The ADUGS-VINS performance across various OpenLORIS scenes.

algorithm to improve the tracking of moving targets even under tough conditions with partial occlusion. Extensive experiments show that ADUGS-VINS effectively manages diverse dynamic objects, significantly enhancing accuracy in complex dynamic environments. Compared to state-of-the-art VIO methods, our approach improves trajectory accuracy, adapts to unseen scenarios, and offers a robust and efficient solution for advancing robotic systems. In the future, we intend to further develop this method to improve the real-time performance of ADUGS-VINS for practical real-world applications.

#### REFERENCES

[1] C. Yu, Z. Liu, X.-J. Liu, F. Xie, Y. Yang, Q. Wei, and Q. Fei, "Ds-slam: A semantic visual slam towards dynamic environments," in *25th IEEE/RSJ International Conference on Intelligent Robots and Systems (IROS)*, ser. IEEE International Conference on Intelligent Robots and Systems, 2018, Conference Proceedings, pp. 1168–1174, times Cited: 489 Liu, Zuxin/GQY-8303-2022; Yu, Chao/HTS-5623-2023; Wei, Qi/JJF-3393-2023; Xie, Fugui/P-8259-2017; Liu, Zuxin/Liu, Zuxin/0000-0001-7412-5074 2153-0858. [Online]. Available: (GotoISI)://WOS:000458872701043

[2] J. Liu, X. Li, Y. Liu, and H. Chen, "Rgb-d inertial odometry for a resource-restricted robot in dynamic environments," *Ieee Robotics and Automation Letters*, vol. 7, no. 4, pp. 9573–9580, 2022, times Cited: 24 Liu, Jianheng/0000-0002-3124-5559; Liu, Yueqian/0000-0002-1994-6408 0 24. [Online]. Available: (GotoISI)://WOS:000831182500036

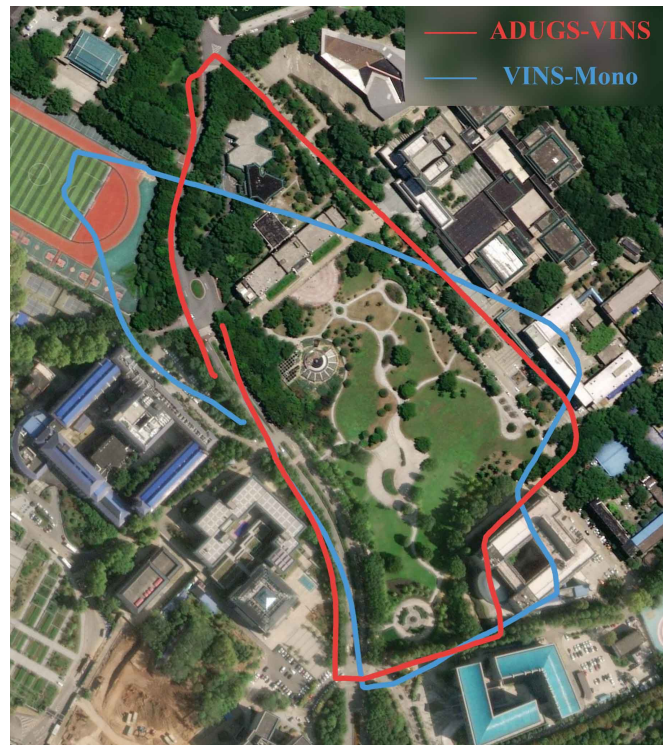


Fig. 9: The estimated trajectories in the real-world environment aligned with the satellite imagery. The red line represents the estimated trajectory obtained from ADUGS-VINS, while the blue line corresponds to the trajectory generated by VINS-Mono.

[3] S. Song, H. Lim, A. J. Lee, and H. Myung, "Dynavins: A visual-inertial slam for dynamic environments," *IEEE Robotics and Automation Letters*, vol. 7, no. 4, pp. 11 523–11 530, 2022.

[4] V. Badrinarayanan, A. Kendall, and R. Cipolla, "Segnet: A deep convolutional encoder-decoder architecture for image segmentation," p. arXiv:1511.00561, November 01, 2015 2015. [Online]. Available: https://ui.adsabs.harvard.edu/abs/2015arXiv151100561B

[5] K. He, G. Gkioxari, P. Dollár, and R. Girshick, "Mask r-cnn," p. arXiv:1703.06870, March 01, 2017 2017, open source; appendix on more results. [Online]. Available: https://ui.adsabs.harvard.edu/abs/2017arXiv170306870H

[6] A. Kirillov, E. Mintun, N. Ravi, H. Z. Mao, C. Rolland, L. Gustafson, T. T. Xiao, S. Whitehead, A. C. Berg, W. Y. Lo, P. Dollár, R. Girshick, and Ieee, "Segment anything," in *IEEE/CVF International Conference on Computer Vision (ICCV)*, ser. IEEE International Conference on

- Computer Vision, 2023, Conference Proceedings, pp. 3992–4003, Kirillov, Alexander Mintun, Eric Ravi, Nikhila Mao, Hanzi Rolland, Chloe Gustafson, Laura Xiao, Tete Whitehead, Spencer Berg, Alexander C. Lo, Wan-Yen Dollár, Piotr Girschick, Ross 1550-5499. [Online]. Available: (GotoISI):/WOS:001159644304024
- [7] A. Bewley, Z. Ge, L. Ott, F. Ramos, and B. Upcroft, “Simple online and realtime tracking,” in *2016 IEEE international conference on image processing (ICIP)*. IEEE, 2016, pp. 3464–3468.
  - [8] C. Campos, R. Elvira, J. J. G. Rodríguez, J. M. M. Montiel, and J. D. Tardós, “Orb-slam3: An accurate open-source library for visual, visual-inertial, and multimap slam,” *IEEE Transactions on Robotics*, vol. 37, no. 6, pp. 1874–1890, 2021.
  - [9] T. Qin, J. Pan, S. Cao, and S. Shen, “A general optimization-based framework for local odometry estimation with multiple sensors,” p. arXiv:1901.03638, January 01, 2019 2019. [Online]. Available: <https://ui.adsabs.harvard.edu/abs/2019arXiv190103638Q>
  - [10] C. Yu, Z. Liu, X. J. Liu, F. Xie, Y. Yang, Q. Wei, and Q. Fei, “Ds-slam: A semantic visual slam towards dynamic environments,” in *2018 IEEE/RSJ International Conference on Intelligent Robots and Systems (IROS)*, Conference Proceedings, pp. 1168–1174.
  - [11] A. I. Mourikis, S. I. Roumeliotis, and Ieee, “A multi-state constraint kalman filter for vision-aided inertial navigation,” in *IEEE International Conference on Robotics and Automation*, ser. IEEE International Conference on Robotics and Automation ICRA, 2007, Conference Proceedings, pp. 3565–+, mourikis, Anastasios I. Roumeliotis, Stergios I. 1050-4729. [Online]. Available: (GotoISI):/WOS:000250915303096
  - [12] M. Bloesch, S. Omani, M. Hutter, R. Siegwart, and Ieee, “Robust visual inertial odometry using a direct ekf-based approach,” in *IEEE/RSJ International Conference on Intelligent Robots and Systems (IROS)*, ser. IEEE International Conference on Intelligent Robots and Systems, 2015, Conference Proceedings, pp. 298–304, times Cited: 554 Siegwart, Roland/A-4495-2008 Siegwart, Roland/0000-0002-2760-7983 2153-0858. [Online]. Available: (GotoISI):/WOS:000371885400043
  - [13] M. Bloesch, M. Burri, S. Omari, M. Hutter, and R. Siegwart, “Iterated extended kalman filter based visual-inertial odometry using direct photometric feedback,” *International Journal of Robotics Research*, vol. 36, no. 10, pp. 1053–1072, 2017, times Cited: 276 Siegwart, Roland/A-4495-2008 Siegwart, Roland/0000-0002-2760-7983 0 332 1741-3176. [Online]. Available: (GotoISI):/WOS:000411059400002
  - [14] P. Geneva, K. Eickenhoff, W. Lee, Y. Yang, and G. Huang, “Opencvins: A research platform for visual-inertial estimation,” in *2020 IEEE International Conference on Robotics and Automation (ICRA)*, 2020, pp. 4666–4672.
  - [15] Y. Fan, T. Zhao, and G. Wang, “Schurvins: Schur complement-based lightweight visual inertial navigation system,” p. arXiv:2312.01616, December 01, 2023 2023, accepted by CVPR2024. [Online]. Available: <https://ui.adsabs.harvard.edu/abs/2023arXiv231201616F>
  - [16] S. Leutenegger, S. Lynen, M. Bosse, R. Siegwart, and P. Furgale, “Keyframe-based visual-inertial odometry using nonlinear optimization,” *International Journal of Robotics Research*, vol. 34, no. 3, pp. 314–334, 2015, leutenegger, Stefan Lynen, Simon Bosse, Michael Siegwart, Roland Furgale, Paul Bosse, Michael/B-7719-2011; Siegwart, Roland/A-4495-2008 Siegwart, Roland/0000-0002-2760-7983 1741-3176. [Online]. Available: (GotoISI):/WOS:000350472800005
  - [17] T. Qin, P. Li, and S. Shen, “Vins-mono: A robust and versatile monocular visual-inertial state estimator,” *IEEE Transactions on Robotics*, vol. 34, no. 4, pp. 1004–1020, 2018.
  - [18] L. Von Stumberg, V. Usenko, and D. Cremers, “Direct sparse visual-inertial odometry using dynamic marginalization,” in *2018 IEEE International Conference on Robotics and Automation (ICRA)*, 2018, pp. 2510–2517.
  - [19] W. Wang, Y. Hu, and S. Scherer, “Tartanvo: A generalizable learning-based vo,” in *Conference on Robot Learning*. PMLR, 2021, pp. 1761–1772.
  - [20] T. Zhou, M. Brown, N. Snavely, and D. G. Lowe, “Unsupervised learning of depth and ego-motion from video,” in *2017 IEEE Conference on Computer Vision and Pattern Recognition (CVPR)*, 2017, pp. 6612–6619.
  - [21] Y. Almalioglu, M. Turan, M. R. U. Saputra, P. P. de Gusmão, A. Markham, and N. Trigoni, “Selfvio: Self-supervised deep monocular visual-inertial odometry and depth estimation,” *Neural Networks*, vol. 150, pp. 119–136, 2022. [Online]. Available: <https://www.sciencedirect.com/science/article/pii/S0893608022000752>
  - [22] Y. Pan, W. Zhou, Y. Cao, and H. Zha, “Adaptive vio: Deep visual-inertial odometry with online continual learning,” in *Proceedings of the IEEE/CVF Conference on Computer Vision and Pattern Recognition (CVPR)*, June 2024, pp. 18 019–18 028.
  - [23] Y. Fan, H. Han, Y. Tang, and T. Zhi, “Dynamic objects elimination in slam based on image fusion,” *Pattern Recognition Letters*, vol. 127, pp. 191–201, 2019, advances in Visual Correspondence: Models, Algorithms and Applications (AVC-MAA). [Online]. Available: <https://www.sciencedirect.com/science/article/pii/S0167865518308523>
  - [24] Y. Sun, M. Liu, and M. Q. H. Meng, “Improving rgb-d slam in dynamic environments: A motion removal approach,” *Robotics and Autonomous Systems*, vol. 89, pp. 110–122, 2017, times Cited: 250 Sun, Yuxiang/HPH-6656-2023; Meng, Max/C-8078-2009; Liu, Ming/AAC-9891-2020; Sun, Yuxiang/; Liu, Ming/ Sun, Yuxiang/0000-0002-7704-0559; Liu, Ming/0000-0002-4500-238X 1 279 1872-793x. [Online]. Available: (GotoISI):/WOS:000392676300010
  - [25] W. Tan, H. Liu, Z. Dong, G. Zhang, and H. Bao, “Robust monocular slam in dynamic environments,” in *2013 IEEE International Symposium on Mixed and Augmented Reality (ISMAR)*, 2013, pp. 209–218.
  - [26] K. Ram, C. Kharyal, S. S. Harithas, K. M. Krishna, and Ieee, “Rp-vio: Robust plane-based visual-inertial odometry for dynamic environments,” in *IEEE/RSJ International Conference on Intelligent Robots and Systems (IROS)*, ser. IEEE International Conference on Intelligent Robots and Systems, 2021, Conference Proceedings, pp. 9198–9205, ram, Karnik Kharyal, Chaitanya Harithas, Sudarshan S. Krishna, K. Madhava Krishna, Madhava/JYO-4800-2024 2153-0858. [Online]. Available: (GotoISI):/WOS:000755125507029
  - [27] J. Li, X. Pan, G. Huang, Z. Zhang, N. Wang, H. Bao, and G. Zhang, “Rd-vio: Robust visual-inertial odometry for mobile augmented reality in dynamic environments,” *IEEE transactions on visualization and computer graphics*, vol. 30, no. 10, pp. 6941–6955, 2024, times Cited: 1 Huang, Gan/0000-0001-8515-2721; Li, Jinyu/0000-0002-5206-8600; Pan, Xiaokun/0000-0002-7438-1665; Zhang, Ziyang/0009-0004-4169-2282; Bao, Hujun/0000-0002-2662-0334; Zhang, Guofeng/0000-0001-5661-8430 0 1 1941-0506. [Online]. Available: (GotoISI):/MEDLINE:38215333
  - [28] M. Runz, M. Bufferl, and L. Agapito, “Maskfusion: Real-time recognition, tracking and reconstruction of multiple moving objects,” in *2018 IEEE International Symposium on Mixed and Augmented Reality (ISMAR)*, 2018, pp. 10–20.
  - [29] B. Bescos, J. M. Fàcil, J. Civera, and J. Neira, “Dynaslam: Tracking, mapping, and inpainting in dynamic scenes,” *IEEE Robotics and Automation Letters*, vol. 3, no. 4, pp. 4076–4083, 2018.
  - [30] R. Khanam and M. Hussain, “YOLOv11: An Overview of the Key Architectural Enhancements,” *arXiv e-prints*, p. arXiv:2410.17725, Oct. 2024.
  - [31] R. E. Kalman, “A new approach to linear filtering and prediction problems,” *Journal of Basic Engineering*, vol. 82D, pp. 35–45, 1960.
  - [32] S. Akhlaghi, N. Zhou, and Z. Huang, “Adaptive adjustment of noise covariance in kalman filter for dynamic state estimation,” in *2017 IEEE Power & Energy Society General Meeting*, July 2017, pp. 1–5.
  - [33] B. D. Lucas and T. Kanade, “An iterative image registration technique with an application to stereo vision,” in *Proceedings of the 7th International Joint Conference on Artificial Intelligence - Volume 2*, ser. IJCAI’81. San Francisco, CA, USA: Morgan Kaufmann Publishers Inc., 1981, p. 674–679.
  - [34] E. Rublee, V. Rabaud, K. Konolige, and G. Bradski, “Orb: An efficient alternative to sift or surf,” in *2011 International Conference on Computer Vision*, 2011, pp. 2564–2571.
  - [35] M. Brown, R. Szeliski, and S. Winder, “Multi-image matching using multi-scale oriented patches,” in *2005 IEEE Computer Society Conference on Computer Vision and Pattern Recognition (CVPR’05)*, vol. 1, 2005, pp. 510–517 vol. 1.
  - [36] K. Minoda, F. Schilling, V. Wüest, D. Floreano, and T. Yairi, “Viode: A simulated dataset to address the challenges of visual-inertial odometry in dynamic environments,” *IEEE Robotics and Automation Letters*, vol. 6, no. 2, pp. 1343–1350, 2021.
  - [37] X. Shi, D. Li, P. Zhao, Q. Tian, Y. Tian, Q. Long, C. Zhu, J. Song, F. Qiao, L. Song, Y. Guo, Z. Wang, Y. Zhang, B. Qin, W. Yang, F. Wang, R. H. M. Chan, and Q. She, “Are we ready for service robots? the openloris-scene datasets for lifelong slam,” in *2020 IEEE International Conference on Robotics and Automation (ICRA)*, 2020, pp. 3139–3145.